

### Protective effect of *Toddaliaasatica* leaf extract on Mild steel in 1.0N HCl

Sangeetha. C<sup>1\*</sup>, Deeparani. P<sup>2</sup>, Selvaraj.S<sup>1</sup>, Kalirajan. K<sup>1</sup>

<sup>1</sup>PG and Research Department of Chemistry, Sri Paramakalyani College, Alwarkurichi-627412,

<sup>2</sup>Aditanar College of Arts and Science, Thiruchendur-628215, Affiliated to ManonmaniamSundaranar University, Abishekapatti, Tirunelveli-627012, Tamil Nadu, India

#### Abstract:

A study has been made on the effect of Novel corrosion inhibitor on mild steel in 1.0N HCl. Commonly deterioration of steel is caused due to various environmental and other chemical factors. It is unavoidable but protectable using inhibition methods. Here the usual inhibitor is replaced by green inhibitors to evade toxicity, easy availability and to minimize the waste. This work seeks out to analyse the dried leaves of *Toddaliaasatica* as an inhibitor on mild steel in 1.0N HCl. The anticorrosive effectiveness of this inhibitor is studied by using non- electrochemical and electrochemical techniques. Non electrochemical studies such as the effect of time (87.6%) and temperature (93.0%) maximum inhibition efficiency achieved at optimum concentration of the inhibitor due to the persistence of protective film formed on the metal surface. Langmuir isotherm best fits the data obtained suggesting the physical adsorption as the adsorption mechanism between the extract and the mild steel substrate. Electrochemical such as potentiodynamic polarization studies proved that extract of *Toddaliaasatica* dried leaves is a cathodic type of inhibitor and 85.12% inhibition efficiency provided by the inhibitor. Charge Transfer Resistance ( $R_{ct}$ ) value increased and also Double-layer capacitance ( $C_{dl}$ ) value decreases by EIS studies. The observed value of inhibitor efficiency at optimum inhibitor concentration is 84.05%. Surface and corrosion product Analysis (EDX/FTIR) were also carried out to determine the corrosion-inhibitive properties of the samples.

**Key Words:** Corrosion, Mild steel, Inhibition, *Toddaliaasatica*

\*Corresponding author Email [id:geetharaja.np@gmail.com](mailto:geetharaja.np@gmail.com)

## Introduction

Today, the impact of corrosion on society and the associated degradation of materials are far-reaching owing in part to the increased complexity and diversity of materials systems, which are subject to environmental extremes. While legacy corrosion concerns remain, advancing technology and the need for global sustainability bring new and emerging corrosion issues whose negative impacts must be minimized through appropriate materials selection, mitigation, monitoring and new materials development. In such a way that corrosion study on the metallic material such as mild steel has become important particularly in acidic media because of the increased industrial applications of acid solutions. Among the acid solutions, hydrochloric acid is one of the most widely used agents during acid pickling, industrial cleaning, acid descaling, oil well acid in oil recovery and the petrochemical processes [1]. To decrease or to prevent the metal from reaction with the media [2] corrosion inhibitors are substances added in small concentrations to a corrosive media. If the corrosion inhibitor has high toxicity, it will inevitably result in secondary pollution [3], hence their use to be restricted and/or prohibited [4]. Therefore, an environmentally friendly corrosion inhibitors are of plant origin has a wide range of sources is a critical requirement in acid pickling and cleaning [5, 6]. This treatment involves the addition of some organic compounds to the acid solution that adsorb at the metal/solution interface forming a compact barrier film. It has been observed that adsorption depends mainly on certain physicochemical properties of the inhibitor group, such as functional groups, heteroatoms (O, N, and S) multiple bonds, electron density at the donor atom, p-orbital character, and the electronic structure of the molecule. Recently many plants studied for their inhibition character such as *Tithonia diversifolia* [7] *Murrayakoenigii* [8] *Luffacylindrica* [9] *Cryptocaryanigra* [10] curcumin [11] *Theobroma cacao* Peel [12] *Terminaliacatappa* [13]. The adequate efficiency of this inhibitor is mainly dependent on its ability to get adsorbed on the metal surface which consists of a replacement of water molecules at a corroding interface. This study aims to evaluate the inhibitive effect of *Toddaliaastalical* leaf extract on the corrosion inhibition of mild steel in hydrochloric acid at ambient temperature using Non-electrochemical and electrochemical measurements.

## Experimental Part Non-Electrochemical Studies Inhibitor

*Toddaliaasatica* leaves [TAL] were collected from western guards. To prepare a stock solution of the plant extract leaves kept under the shadow, ground to powder form. Approximately 100g of the powder immersed in alcohol for about 48hrs. Then alcohol solvent was removed by the evaporation process and the pure TAL extract was collected. The stock of the extract obtained was used in preparing different concentrations of the extract by dissolving in 1.0N HCl respectively.

### Preparation of test Specimen

Rectangular specimen of mild steel was mechanically pressed, cut to form different coupons, each of dimension exactly 20cm<sup>2</sup> (5x2x2cm<sup>2</sup>) abraded with an emery wheel of 80 and 120 and degreased using trichloroethylene, washed with distilled water, cleaned and dried, then stored in desiccator for throughout our present study.

### Non-Electrochemical and Electrochemical Methods

Initially, mild steel specimen weighed and immersed in 100ml of test solution for 24 to 360 hours at room temperature in the presence and absence of TAL inhibitor. The temperature studies carried out range from 303K to 333K for an hour. At the end of the designated period, specimens were washed and the final weight was recorded. The experiment was conducted in triplicates to avoid the error during analysis. The data obtained inputted in a formula and thus the corrosion rates, degree of surface coverage and inhibition efficiency (IE %) calculated as follows,

$$\text{Corrosion rate} \left( \frac{\text{mm}}{\text{y}} \right) = \frac{87.6 \times W}{DAT} \text{ --- (1)}$$

W=Mass loss (mg), D= Density(gm/cm<sup>3</sup>), A= Area of specimen(cm<sup>2</sup>), T=Time in hours

$$\text{IE}\% = \frac{w_1 - w_2}{w_1} \times 100 \text{ --- (2)}$$

$$\theta = \frac{w_1 - w_2}{w_1} \text{ --- (3)}$$

Where, W<sub>1</sub> and W<sub>2</sub> are the corrosion rate in the absence and presence of the ESL extract.

### Electrochemical Studies

Electrochemical measurements such as Potentio-dynamic polarization and electrochemical impedance spectroscopy (EIS) were carried out using CHI660E Instrument designed with three electrode cell for electrochemical corrosion tests. The data of electrochemical measurements started

after 30 min from immersing the working electrode in the acidic solution that's time is to allow steady state potential to stabilize. The polarizing potential applied between the reference electrode (RE) and the working electrode (WE) at any prescribed value to measure the density of the current on the counter electrode (CE). The polarization curve obtained from potentiodynamic method. The inhibition efficiency (%) was calculated using  $I_{corr}$  values both in the absence and presence of inhibitor.

$$IE\% = \frac{I_{Corr}(blank) - I_{Corr}(inh)}{I_{Corr}(blank)} \quad \text{--- (4)}$$

Where  $I_{corr}$  (blank) and  $I_{corr}$ (inh) are the corrosion current density values of mild steel in the absence and presence of inhibitors.

Impedance spectroscopy measurements were carried out with an AC signal of 5mV amplitude and with a frequency range of 1 to 10<sup>6</sup>Hz. By using Zsimp win software analyst, all the data of impedance were fitted to an appropriate equivalent circuit (EC). The Charge Transfer Resistance obtained from the diameter of the semicircle of the Nyquist plot. The inhibition efficiency (IE %) calculated using the following equation

$$IE\% = \frac{R_{ct}(inh) - R_{ct}(Blank)}{R_{ct}(inh)} \quad \text{--- (5)}$$

Where,  $R_{ct}$ (inh)=Charge Transfer Resistance with inhibitor

$R_{ct}$  (blank)= Charge Transfer Resistance without inhibitor

All the measurements were carried out at room temperature in air-saturated solutions under unstressed conditions. To test the reliability and

reproducibility of the measurements, triplicate experiments were performed in each case of the same conditions.

### EDX Analysis

Compositions of all elements present on the surface of the specimen, before and after immersion identified by Energy Dispersive X-ray spectroscopy (EDX) using the Oxford Instrument Model - INCA PentaxFET. The energy of an acceleration beam employed was 20kV

### FTIR

The corrosion product was analyzed using Fourier transform infrared spectroscopy (FT-IR) model Jasco within the range of 4000 – 400cm<sup>-1</sup>. All FTIR spectra were corrected to identify the functional groups and various elements present.

### Scanning Electron Microscope (SEM)

Surface morphological examination of Mild steel specimen after immersion in acid solution containing optimum concentration of inhibitor and blank was performed by Model: Jeol – JSM 6390 scanning electron microscope (SEM).

### Non-electrochemical studies

#### Effect of immersion time

The observed results (Table-1) indicate that the percentage of inhibition efficiency and degree of surface coverage increased with the increases of inhibitor concentration. The achievement of maximum inhibition (87.6%) efficiency may be due to the adsorption of active components of plant extract (alkaloids, tannins, saponins, flavonoids) [14] on the mild steel surface by the interaction of  $\pi$ -electrons or lone pair electron of heteroatoms (N and O).

**TABLE I. Calculated Values of corrosion rate and inhibition efficiency (%) of different concentration on TAL on mild steel in 1.0 N HCl**

Con ppm	24 hrs			72 hrs			120hrs			240hrs			360 hrs		
	CR (mm/y)	$\Theta$	%IE	CR (mm/y)	$\Theta$	%IE	CR (mm/y)	$\Theta$	%IE	CR (mm/y)	$\Theta$	%IE	CR (mm/y)	$\Theta$	%IE
0	14.74	-	-	5.457	-	-	3.367	-	-	1.823	-	-	1.24	-	-
10	12.77	0.133	13.3	4.923	0.097	9.7	3.037	0.097	9.7	1.435	0.212	21.2	1.07	0.133	13.3
50	11.10	0.247	24.7	4.079	0.252	25.2	2.410	0.284	28.4	1.126	0.382	38.2	0.857	0.308	30.8
100	5.039	0.658	65.8	3.452	0.367	36.7	2.280	0.322	32.2	0.703	0.614	61.4	0.772	0.377	37.7
500	3.25	0.779	77.9	2.910	0.466	46.6	0.673	0.8	80	0.647	0.644	64.4	0.479	0.613	61.3
1000	2.85	0.806	80.6	0.921	0.831	83.1	0.505	0.851	85.1	0.232	0.872	87.2	0.153	0.876	87.6

**Effect of Temperature**

The corrosion parameter of mild steel in 1.0N Hydrochloric acid containing various concentrations of *TAL* inhibitor with the temperature ranging from 303 to 333K after one hour immersion time represented in Table- 2.

The maximum of 93.0 % of inhibition efficiency was attained at 303K, this temperature consider as a optimum temperature. The decreasing inhibition performance on raising the temperature (333K) of a solution may be due to the increasing of the inhibitor molecules mobility and desorption of the adsorbed molecules lead to decreasing the interaction between inhibitor molecules and mild steel surface. Thus, there may be [15] a stable thin film formation over the metal surface.

**Activation Parameters**

Activation parameters in the absence and presence of *TAL* extract give an insight in to the inhibitor adsorption mechanism by calculating the  $E_a$  values of the corrosion reaction with and without *TAL* extract. The apparent activation energy can be calculated using the Arrhenius famous equation which evaluates the temperature dependency to the corrosion rate:

$$CR = A_{\exp(-E_a/RT)} \quad \text{--- (6)}$$

$E_a$  is the apparent activation energy,  $A$  is constant,  $R$  is the universal gas constant ( $R = 8.314 \text{ j mol}^{-1} \text{ K}^{-1}$ ) and  $T$  is the absolute temperature.

Straight line obtained by plotting  $\log CR$  versus  $1/T$  (Fig: 1a) and the activation energy can be calculated from the slope. The corresponding values of the apparent activation energy are listed in Table -3. Analysis of temperature dependence of inhibitor concentration as well as comparison of activation energy gives insight into the possible mechanism.

An increase in inhibition efficiency with rise in temperature, with analogous decrease in corrosion activation energy in the presence of inhibitor compared to its absence, is frequently interpreted as being suggestive of formation of chemically adsorption film. Whereas a decrease in inhibition efficiency with rise in temperature, with corresponding increase in corrosion activation energy in the presence of inhibitor compared to its absence, is recognized as physical adsorption mechanism. Moreover Chemical adsorption, in this case, requires higher activation energy (40 to 800kJ/mol) than physical adsorption (5 to 40kJ/mol). On the surface, chemical adsorption forms a monolayer film. As a result, the reaction rate stays low even as the concentration increases, and the activation energy changes very little [16]. However, in physical adsorption, the thickness of the film increased as the concentration increased, influencing the activation energy. It is apparent from Table.3 that the activation energy is about 24.56-41.013kj/mol. It's also worth noting that the activation energy of an inhibited mechanism is greater than that of an uninhibited process. Furthermore, even if the activation energy declines after a certain concentration, the value remains higher than the blank operation. As a result, the findings indicate that *Toddaliaasatica* leaf extract adsorption on the metal surface is due to physical adsorption. Since the inhibitor molecules are bound to the metal surface by weak bonds such as van der Waals forces, hydrogen bonding, or hydrophobic interactions, the efficiency of physical adsorption decreases as the temperature issues [17]. Physical adsorption is supported by the fact that the *Toddaliaasatica* leaf extract's efficiency decreases as the temperature increases.

**TABLE II. Effect of temperature on the corrosion of mild steel in the presence of various concentration of *TAL* inhibitor in 1.0N HCl**

Con ppm	Corrosion rate(mm/y)			Inhibition Efficiency (%)		
	303 K	313K	333 K	303K	313K	333K
0	71.06	128.23	172.82	-	-	-
10	42.30	84.72	120.17	40.44	33.96	30.47
50	22.10	65.76	98.74	68.0	48.74	42.87
100	6.35	25.06	51.05	91.0	80.46	70.50
500	5.29	16.78	28.0	92.0	86.92	83.89
1000	4.68	11.22	17.68	93.0	91.25	89.79

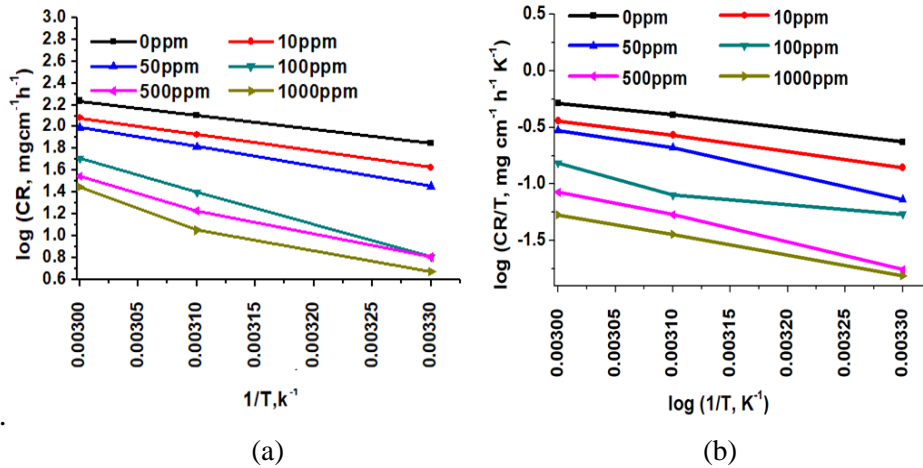


**Fig 1(a,b).** Arrhenius and Transition plot for mild steel corrosion in 1.0N HCl in the absence and presence of different concentration of TAL.

**TABLE III: Activation and Transition state parameters of TAL in 1.0N HCl on mild steel.**

Conc ppm	Arrhenius parameters		Transition state parameters		
	log A	Ea (kJ/mol)	$\Delta S$ (j / k mol)	$\Delta H$ (kj/ mol)	$Q_{ads}$ (kj/mol)
0	6.095	24.56	83.685	9.627	-
10	6.613	28.931	84.204	11.506	-95.570
50	7.421	34.68	86.190	17.197	-85.002
100	10.74	57.652	88.703	11.780	-25.162
500	7.87	41.013	86.346	19.163	-69.094
1000	7.00	36.762	84.597	14.907	-37.643

**Transition Parameter**

Transition parameters, such as enthalpy and entropy of the corrosion process were evaluated from the effect of temperature. A transition formulation of the Arrhenius equation (Eq. 7) can be used:

$$CR = \frac{RT}{Nh} \exp\left(\frac{\Delta S}{R}\right) \exp\left(\frac{\Delta H}{R}\right) \dots (7)$$

where  $h$  is Planck’s constant,  $N$  is Avogadro’s number,  $\Delta S$  is the entropy of activation,  $\Delta H$  is the enthalpy of activation,  $T$  is the absolute temperature and  $R$  is the universal gas constant.

Fig: 1b shows the variation of  $\log (CR/T)$  against  $1/T$  for TAL extract. Straight lines are obtained with a slope of  $(-\Delta H / 2.303 \times RT)$  and an intercept of  $(\log RT/Nh + \Delta S / 2.303 \times R)$  from which the values of  $\Delta H$  and  $\Delta S$  calculated, respectively.

The positive value of  $\Delta S$  (83.685-84.597 kJ mol<sup>-1</sup>) shows the increased randomness at the metal/solution interface during the adsorption of inhibitor molecules onto the metal surface.

Inspection of these above data reveals that the  $\Delta H$  values for the dissolution reaction of mild steel

in 1.0N HCl in the presence of inhibitor are higher (14.907 kJ mol<sup>-1</sup>) than that in the absence of an inhibitor (9.627 kJ mol<sup>-1</sup>). This indicates the barrier to the corrosion reaction increased and the corrosion rate of the metal decreased. This was due to the adsorption of inhibitor molecules present in the TAL extract on the metal surface. The value of  $\Delta H$  was positive, which indicates that the dissolution of the mild steel was an endothermic process, which requires more energy to reach an effective or equilibrium state.

**Heat of Adsorption**

The heat of adsorption on the surface of metals in the presence of plant extract in an acid environment is calculated by the following equation (8).

$$Q_{ads} = 2.303 R \left[ \log \left( \frac{\theta_2}{1-\theta_2} \right) - \log \left( \frac{\theta_1}{1-\theta_1} \right) \right] \frac{T_2 T_1}{T_2 - T_1} \dots (8)$$

The calculated  $Q_{ads}$  values (Table-4) are ranged from -95.570 to -37.643 kJ/mol indicating that the

adsorption of ethanol extract of *TAL* on mild steel surface is endothermic.

### Adsorption Studies

Adsorption isotherm is very important to determine the reaction mechanism, for this the linear relation between the degree of surface coverage ( $\theta$ ) and inhibitor concentration ( $C$ ) must be found. Attempts were made to fit the  $\theta$  values to various isotherms such as Langmuir Frumkin, Temkin, Flory–Huggins, and El Awady. Average regression coefficient ( $R^2$ ) values for Langmuir (0.9849), El-Awady (0.8543), Frumkin (0.8332), Temkin (0.7923), Freundlich (0.7525), Florry-Huggins (0.7296). The best fit was obtained with the Langmuir isotherm, by plotting  $\log C/\theta$  against  $\log C$  at 303, 313

and 333 K (fig: 2). where the correlation coefficients ( $R^2$ ) were found to be approximately one.

The Langmuir isotherm is based on the assumption that all adsorption sites are equivalent and that particle binding occurs independently from nearby sites, whether occupied or not. It is given as equation 9 [6]

$$\log \frac{C}{\theta} = \log C - \log K \quad \text{--- (9)}$$

Where  $C$  is the concentration of the inhibitor in the bulk electrolyte,  $\theta$  is the degree of surface coverage of the inhibitor and  $K$  is the equilibrium constant of adsorption of the inhibitor adsorption process.

The slopes of the straight lines are also near unity, suggesting that adsorbed surfactant molecules form a monolayer on the mild steel surface and there is no interaction among the adsorbed inhibitor molecules.

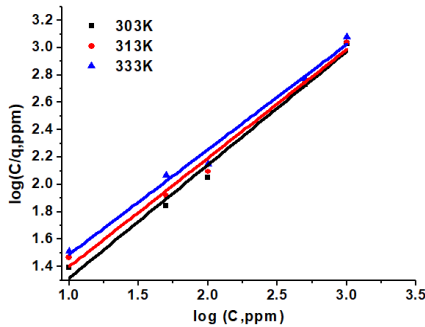


**Fig 2. Langmuir plot of *TAL* Inhibitor on mild steel in 1.0N HCl**

The values of Gibbs free energy of adsorption  $\Delta G_{ads}$  calculated from the values of the equilibrium constant of adsorption ( $K_{ads}$ ) obtained from the Langmuir adsorption isotherm above using equation 9 and also presented in Table 4:

$$\Delta G_{ads} = -2.303 RT \log(55.5K) \quad (10)$$

Where  $\Delta G$  is the free energy of adsorption;  $R$  is the gas constant;  $K$  is the equilibrium constant of adsorption and  $T$  is the temperature. From the results presented, it can be said that the negative values of  $\Delta G$  (47.20 to 47.366 kJ/mol) obtained indicate that the adsorption process is spontaneous.

### Potentiodynamic Polarisation Spectroscopy

The effect of *TAL* extract on the anodic and cathodic polarization behaviour of mild steel in

1.0N HCl solution has been studied using polarization measurements and the recorded Tafel plots for various concentrations are shown in Fig: 3. The respective electrochemical parameters obtained from the plots are given in Table-5. The diminution of  $I_{corr}$  is more evident because a higher amount of *TAL* extract molecules in the corrosive medium compete for blocking the active sites from the presence of aggressive ions ( $Cl^-$ ) and water molecules.

However, some active sites cannot be protected due to the presence of inclusions, grain boundary defects and the topography of the steel surface. Also  $b_a$  and  $b_c$  gradually decrease with increasing the inhibitor concentration, reflecting the decrease of the current densities (i.e. decrease in the corrosion rate) shown in table-5.

**TABLE IV. Adsorption Isotherms values for mild steel in 1.0N HCl with different concentration of *TAL* extract**

Isotherm	$R^2$	Temp K	Slope	$-\Delta G$ kJ/mol
Langmuir	0.9849	303	0.7677	47.204
		313	0.8281	43.601
		333	0.7947	47.366
El-Awady	0.8543	303	0.8087	12.997
		313	0.8369	14.301
		333	0.6408	13.620

**TABLE V. Polarisation Parameters of the mild steel in 1.0N HCl Containing TAL extract**

Conc. (ppm)	-E <sub>corr</sub> (mV)	b <sub>a</sub> (V dec <sup>-1</sup> )	b <sub>c</sub> (V dec <sup>-1</sup> )	I <sub>corr</sub> (mA cm <sup>-2</sup> )	IE (%)	CR
0	387.4	9.804	13.22	1041	-	996.4
10	408.5	9.669	12.775	519.9	50.05	67.01
50	460.7	9.337	12.585	358.7	65.54	33.45
100	474.4	8.585	12.134	353.0	66.09	23.08
500	476.9	3.856	11.472	269.5	74.11	22.71
1000	479.9	3.463	8.412	154.9	85.12	17.34

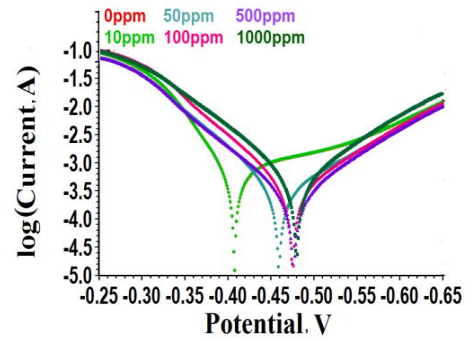


**Fig. 3 Polarisation curve of TAL leaf extract in 1.0N HCl on mild steel**

The  $E_{corr}$  displaced to more positive values within the interval ranging from -387.4 to -479.9mV at the evaluated concentrations; then, the TAL extract can be classified as anodic or cathodic inhibitor being preferably adsorbed on the cathodic zones of the evaluated steel [18]. The inhibition efficiency (Eq-4) increased from 50 to 85%.

**Impedance Studies**

The inhibition processes of the *Todaliaasatica* leaves extract studied using electrochemical impedance spectroscopy technique for mild steel in 1.0N HCl in the presence and absence of various concentrations of TAL extract at 30°C are presented in Figure 4.

The high frequency capacitive loop is related to the charge transfer of the corrosion process and double layer behaviour. On the other hand, the low frequency capacitive loop may be due to the relaxation process obtained by adsorption of inhibitor species [19] and the re-dissolution of the passivated surface at low frequencies [20] on the electrode surface. These high frequency loops are not perfect semicircles which can be attributed to the frequency dispersion as a result of the roughness and inhomogeneous of the electrode surface [21].

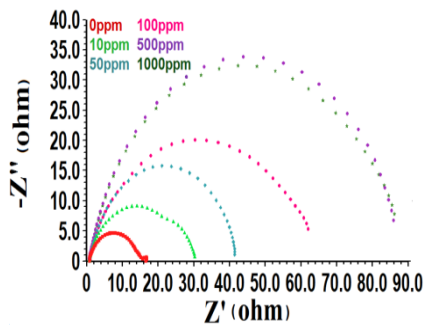


**Fig 4. Nyquist plot of mild steel in 1.0N HCl with different concentrations of TAL**

Furthermore, the diameter of the capacitive loop in the presence of an inhibitor is bigger than that in the absence of an inhibitor (blank solution). This indicates that the impedance of the inhibited substrate increases with TAL extract concentration. The EIS results of high frequency capacitive loops are simulated by the equivalent circuit (Fig. 5) to pure electric models that could verify or rule out mechanistic models and enable the calculation of numerical values corresponding to the physical and/or chemical properties of the electrochemical system under investigation [22]. It is worth mentioning that the double layer capacitance ( $C_{dl}$ ) value is affected by imperfections of the surface, and that this effect is simulated via a constant phase element (CPE).

The constant phase element is composed of the component  $Y_0$  and coefficient  $n$ . Parameter  $Y_0$  describes the non-ideal behaviour of the capacitance, and the parameter  $n$  quantifies different physical phenomena like surface heterogeneousness resulting from surface roughness, inhibitor adsorption, porous layer formation, etc. So the capacitance can be expressed by the following equation,

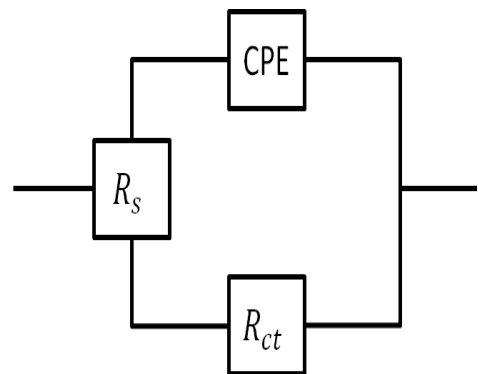


**Fig 5. Equivalent Circuit**

$$Z_{CPE} = \frac{1}{Y_0(j\omega)^n} \text{ --- (11)}$$

Where  $j$  is the imaginary number,  $Y_0$  is the frequency independent real constant,  $\omega = 2\pi f$  is the angular frequency (rad/s),  $f$  is the frequency of the applied signal, and  $n$  is the CPE exponent.

The Double layer capacitance calculated using the following expression

$$C_{dl} = \frac{1}{2\pi F_{max} R_{ct}} \text{ --- (12)}$$

The results of the correlation analysis of individual electrical elements such as values of the fitting quality parameter ( $R_{ct}$ ,  $C_{dl}$ ,  $n$ ) using Zsimp win software were presented in Table 6. Charge Transfer Resistance increased from 14 to 87.81  $\Omega\text{cm}^{-2}$  with the increasing of *TAL* extract concentration indicates that the coverage of the inhibitor increases, while the  $C_{dl}$  decreased with the increases of the inhibitor concentration which is due to the increase in the thickness of the protective layer at higher concentration [23-28]. This decreased  $C_{dl}$  values recertified the physical adsorption. The inhibition efficiency increased shows the better inhibition performance of *TAL* extract.

The Bode and phase angle plots obtained at different concentrations of *TAL* extract are shown in Figures: 6a & 6b respectively. Bode plots provide the impedance value with respect to frequencies. Bode curves show higher impedance values at lower frequencies for higher inhibitor concentration respectively. This confirms the higher shielding effect of inhibitors molecules on the mild steel surface, which is correlated to the adsorption of the *TAL* compounds over the metal surface. According to the phase angle plots (Fig: 6b), an increase in the concentration of inhibitors in the electrolyte medium results in a rise of the phase angles closer to 90°, which signifies more inhibitive performance due to the adsorption of the inhibitor molecules on the surface of mild steel at higher concentrations.

### EDX Spectroscopy

EDX spectroscopy was used to determine the elements present on the mild Steel surface in the presence and absence of inhibitor (Figs: 7 a, b). In the absence of inhibitor molecules, the spectrum may conclude that the existence of elements presents in the metal and environments. However, in the presence of the concentrations of the inhibitor, the hetero atoms like Oxygen and sulphur elements are found to be present in the corrosion product on the metal surface. It clearly indicates that these hetero atoms present in the inhibitor molecules may involve

**TABLE VI. EIS Parameters for the corrosion of mild steel in 1.0N HCl containing *TAL***

Electrolyte (ppm)	$R_{ct}$ ( $\Omega\text{ cm}^{-2}$ )	$f_{max}$ (Hz)	$C_{dl}$ ( $\mu\text{Fcm}^{-2}$ )	$n$	IE (%)
0	14	7.3	0.0155	0.83	-
10	29.66	14.26	0.0037	0.84	52.79
50	41.12	21.12	0.0018	0.85	65.95
100	64.06	30.49	0.00081	0.85	78.14
500	87.18	42.69	0.00042	0.86	83.94
1000	87.81	44.19	0.00041	0.86	84.05

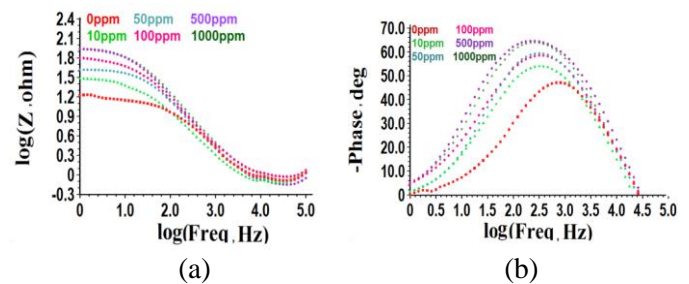


**Fig 6(a,b). EIS studies of mild steel in 1.0N HCl with different concentrations of *TAL***  
 (a)Bode plot, (b) Phase angle plots.

the film formation with the metal ion during the adsorption process and prevent the further dissolution of metal against corrosion.

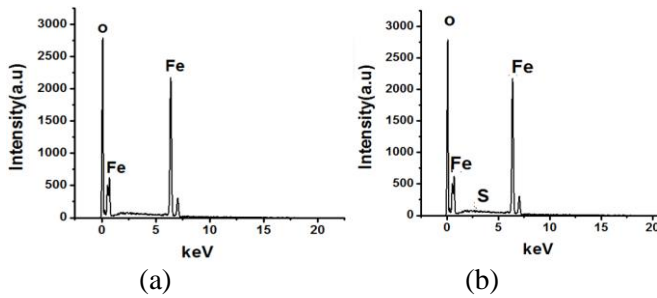
### Scanning Electron Microscope (SEM) Image

Image of the surface morphology of mild Steel before and after immersion in 1.0NHCl in the presence and absence of *TAL* extract is represented in Fig:8(a-c). The surface morphology of mild steel in the absence of an inhibitor shows that the severe damage on the metal surface leads to pitting type of corrosion (Fig:8b). However, in the presence of *TAL* extract (Fig:8c), the almost smooth and completely covered images confirm the film formation which could effectively safeguard the surface from corrosive environments.

### FTIR

The FT-IR spectra of plant extract and corrosion products obtained from the mild steel surface are shown in Fig: 9. Spectra of *TAL* leaf extract exhibited peak at 2922, 2854, 1730, 1448, 1375,1230,1165,1070,1035,831 $\text{cm}^{-1}$ . FTIR spectrum of the film formed by the presence of *TAL* extract on the metal surface shows a prominent peak at 3275, 1621, 1105, 1028 $\text{cm}^{-1}$ . It is seen from the spectrum that the  $>\text{OH}$  stretching in *TAL* extract of frequency shifted from 3376 $\text{cm}^{-1}$  to 3275 $\text{cm}^{-1}$ . The peak at 1707 $\text{cm}^{-1}$  shifted to 1621 $\text{cm}^{-1}$  corresponding to





**Fig 7(a,b). EDX spectrum of the corrosion product and corrosion product in the presence of TAL leaf extract on Mild steel surface in 1.0N HCl**  
 (a) Bode plot, (b) Phase angle plots.

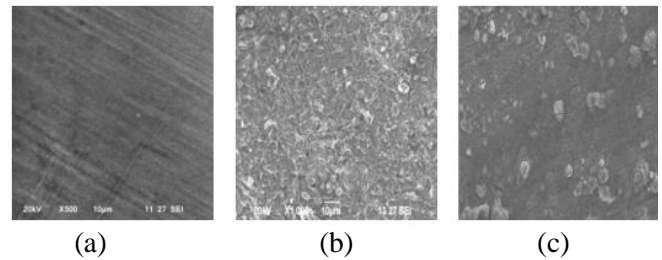


**Fig:8(a -c) SEM image of the Polished Carbon Steel surface, Before and After immersed in 1.0N Hydrochloric acid with TAL extract respectively.**

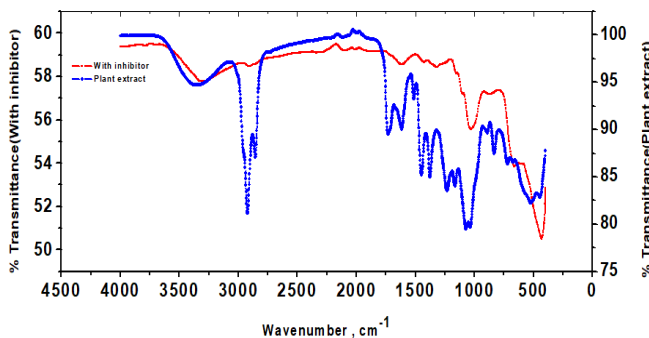


**Fig 9. FTIR spectra of corrosion product in the presence of TAL leaf extract in 1.0N HCl on mild steel**

>C=O stretching vibration. Also stretching in TAL extract of frequency shifted from  $1161\text{cm}^{-1}$  to  $1105\text{cm}^{-1}$ . The band shifted from  $1027\text{cm}^{-1}$  to  $1028\text{cm}^{-1}$  respectively. Some functional groups were missing in the spectra of the corrosion product suggesting that the adsorption of the inhibitor on the surface of the mild steel might have occurred through the missing bands.

## CONCLUSION

Toddaliaasatica leaf extract shows an excellent and efficient inhibitor on mild steel in 1.0N HCl environment. Inhibition efficiency increased with increases of inhibitor concentration and maximum inhibition efficiency for the extract achieved 93%. The inhibitor follows Langmuir adsorption isotherm ( $R^2=0.99$ ). The values of apparent activation energy increased ( $24.56\text{ kJ/mol} - 41.013\text{ kJ/mol}$ ) with the increase of inhibitor concentration shows that the physisorption based mechanism. The positive value of the enthalpy ( $9.627\text{ to } -14.907\text{ kJ/mol}$ ) of adsorption indicates that the reaction of the TAL is endothermic. Polarization measurement results revealed that  $I_{\text{corr}}$  value decreased from  $1041\text{ to } 154.9\text{ mAcm}^{-2}$  with increase of inhibitor concentration.  $E_{\text{corr}}$  values deviate from  $-387.4\text{ to } 479.9\text{ mV}$ , suggest that the TAL extract behaves as a

cathodic type of inhibitor and attained a maximum of 85.12% IE. Impedance studies show that the Charge Transfer Resistance ( $R_{\text{ct}}$ ) increased from 14 to  $87.81\text{ }\mu\text{m}^2$  with increases of inhibitor concentration and achieved a maximum of 84.05% IE. The analysis of corrosion composite by using EDX, SEM, and FT-IR revealed that the formation of the strong protective thin film formed on the surface.

## References

1. A.H. Ostovari, S.M. Peikari, S.R. Shadzadeh, S.J. Hashemi, Corros. Sci. 51 (2009) 1935. ([Doi 10.1016/j.corsci.2009.05.024](https://doi.org/10.1016/j.corsci.2009.05.024))
2. A.Singh, Eno E. Ebenso, and M. A. Quraishi, Int. J. Corros., 2012 (2012) (<https://doi.org/10.1155/2012/897430>)
3. E Rodriguez-Clemente, JG Gonzalez-Rodriguez, G Valladarez and GF Dominguez-Patiño, Int. J. Electrochem. Sci., 6 (2011) 6360.
4. A.Singh, Eno E. Ebenso, and M. A. Quraishi, Int. J. Corros., 2012 (2012). (<https://doi.org/10.1155/2012/897430>)
5. E Rodriguez-Clemente, JG Gonzalez-Rodriguez, G Valladarez and GF Dominguez-Patiño, Int. J. Electrochem. Sci., 6 (2011) 6360.
6. Xia Wang\*, Huan Jiang\*, Dai-xiong Zhang, Li Hou, Wen-jie Zhou, Int. J. Electrochem. Sci., 14 (2019) 1178 – 1196. ([doi: 10.20964/2019.02.06](https://doi.org/10.20964/2019.02.06))
7. P.Divya S.Subhashini A.Prithiba R.Rajalakshmi, 18, Part 4, (2019) 1581-1591.
8. K. Yadav, A. Gupta, S. N. Victoria, R. Manivannan,, Indian J. Chem. Technol., 25 (2018) 94-100. (<http://nopr.niscair.res.in/handle/123456789/43613>)
9. O.O. Ogunleye, a A.O. Arinkoola, a, c, \* O.A. Eletta, b O.O. Agbede, a Y.A. Osho, 6(1) (2020) 03205. doi: [10.1016/j.heliyon.2020.e03205](https://doi.org/10.1016/j.heliyon.2020.e03205)
10. Mas Faiz<sup>a</sup>, Azeana Zahari<sup>\*a</sup>, Khalijah Awang<sup>a</sup> and Hazwan Hussin, RSC Adv., 10(2020) 6547-6562
11. M. Abdallah, Hatem M. Altass, B. A. AL Jahdaly & M. M. Salem, 11(1) (2018) 189-196. (<https://doi.org/10.1080/17518253.2018.1458161>)

12. YuliYetri, Gunawarman, Emriadi and NovesarJamarun. International Conference on Biological, Chemical and Environmental Sciences (BCES-2014) June 14-15, 2014 Penang (Malaysia). (<http://dx.doi.org/10.15242/IICBE.C614002>)
13. J.O. Madu<sup>1</sup>, C. Ifeakachukwu<sup>1</sup>, U. Okorodudu<sup>1</sup>, F.V. Adams<sup>1,2\*</sup>, I.V. Joseph, Journal of Physics, 1378 (2019). International Conference on Engineering for Sustainable World Conference Series, Journal of Physics, IOP Publishing, 1378, (2019) 022092 ([doi:10.1088/1742-6596/1378/2/02209](https://doi.org/10.1088/1742-6596/1378/2/02209))
14. IB.Obot, SA. Umoren, NO. Obi-Egbedi J Mater Environ Sci, 2(2011) 60–71
15. LM. Vracar, DM. Drazic, Corros Sci 44 (2002), 1669–1680. ([https://doi.org/10.1016/S0010-938X\(01\)00166-4](https://doi.org/10.1016/S0010-938X(01)00166-4))
16. S. F. Desouza, S. R. Goncalves, A. spinelli, Assessment of caffeine Adsorption onto mild steel surface as an Eco-friendly corrosion inhibitor. *J. Brazil Chem. Soci.* 25 (2014) 81-90.
17. A. Popova, E. Sokolova, S. Raicheva, M. Christov, AC and DC study of the temperature effect on mild steel corrosion in acid media in the presence of benzimidazole derivatives, Corros. Sci. 45 (2003) 33–58.
18. N. Labjar, M. Lebrini, F. Bentiss, N.E. Chihib, S. El Hajjaji, C. Jama, Mater. Chem. Phys. 119 (2010) 330–336. (<https://doi.org/10.1016/j.matchemphys.2009.09.006>)
19. M. Lagrenee, B. Mernari, M. Bouanis, M. Traisnel, F. Bentiss, Corros. Sci. 44 (2002) 573–588. ([https://doi.org/10.1016/S0010-938X\(01\)00075-0](https://doi.org/10.1016/S0010-938X(01)00075-0))
20. A.K. Singh, M.A. Quraishi, Corros. Sci. 52 (2010) 152–160. (<https://doi.org/10.1016/j.corsci.2009.08.050>)
21. M. Lebrini, M. Lagrenee, H. Vezin, M. Traisnel, F. Bentiss, Corros. Sci. 49 (2007) 2254–2269. (<https://doi.org/10.1016/j.corsci.2006.10.029>)
22. A.R.S. Priya, V.S. Muralidharam, A. Subramania, Corrosion 64 (2008) 541–552. (<https://doi.org/10.5006/1.3278490>)
23. P. Bommersbach, C. Alemany-Dumont, J.P. Millet, B. Normand, Electrochim. Acta 51 (2006) 4011–4018. (<https://doi.org/10.1016/j.electacta.2005.11.020>)
24. N. M. EL Basony et al, *RSC Adv.* 9, 10473 (2019). (doi: [10.1039/C9RA00397E](https://doi.org/10.1039/C9RA00397E))
25. A. S. Fouda *et al*, Aqueous Extract of Juniperus as a Green Corrosion Inhibitor for Mild Steel (MS) in Sulfamic Acid (NH<sub>2</sub>SO<sub>3</sub>H) Solutions, *Protection of Metals and Physical Chemistry of Surfaces*, 2018.
26. Sylvester Obaike Adejo et al, Journal of Advances in chemistry Vol 15, No 2 (2018). (<https://doi.org/10.24297/jac.v15i2.7883>)
27. P. Geethamani, Corrosion Inhibition and Adsorption Properties of Mild Steel in 1 M Hydrochloric Acid Medium by Expired Ambroxol Drug, *Journal of Bio and Tribo-Corrosion* (5)16, (2019). (<https://doi.org/10.1007/s40735-018-0205-5>)
28. Omar Benali, Inhibition of acid corrosion of mild steel by *Anacyclus pyrethrum* L. Extracts, *Res Chem Intermed* 40:259–268, (2014) (<https://doi.org/10.1007/s11164-012-0960-8>)